AIAA 2009-2481

Sandwich Panels with Stepped Facings

Cody H. Nguyen[1], K. Chandrahsekhara[2] and Victor Birman[2,3]

[1] *Boeing, 163 J.S. McDonnell Blvd St. Louis, Missouri*

[2] *Department of Mechanical and Aerospace Engineering,* [3] *Engineering Education Center*

Missouri University of Science and Technology

(Formerly University of Missouri-Rolla)

One University Blvd.

St. Louis, Missouri 63121

Abstract

Sandwich panels have been developed to either design a lighter structure capable of carrying prescribed loads or to increase the load-carrying capacity subject to limitations on the weight. The major load-carrying elements of a sandwich structure are its facings, while the core primarily serves to resist transverse shear loads, enhance local strength and stability of the facings, and combine two facings into a single structural system. The facings being subject to bending and in-plane tensile/compressive loads and to in-plane shear, their strength and stiffness are paramount to the sandwich structure. In the present paper we investigate advantages of so-called "stepped" facings with geometry modified to locally enhance the strength and stiffness at strategically important locations with a minimum effect on the weight. We illustrate that sandwich designs with stepped facings can be attractive in static problems concerned with strength and stability, while their advantage in situations where it is necessary to increase the fundamental frequency of the panel is less pronounced.

Nomenclature

A_{ii}	= extensional stiffnesses
C_{ij}	= elements of stiffness tensor in the stress-strain relationships
D_{ij}	= bending stiffnesses
h	= panel thickness
k	= shear correction factor
q	= lateral pressure
$u_0,\ v_0$	= middle plane displacements in the x- and y-directions, respectively
w	= deflection of the panel

[1]Engineer, 163 J.S. McDonnell Building, Boeing
[2]Professor of Mechanical and Aerospace Engineering, Associate Fellow of AIAA
[3]Professor of Mechanical Engineering, Associate Fellow of AIAA

ε = axial strain
γ = shear strain
σ = axial stress
τ = shear stress
ψ_x, ψ_y = rotations of the cross section in the xz and yz planes, respectively

1. Introduction

Sandwich panels usually have to satisfy a number of requirements to their strength, stiffness, stability and dynamic properties. These requirements can be met by enhancing the stiffness of the facings. This stiffness can be improved using one of the following methods:

1. Stiffer facing material with higher strength;

2. Functionally graded composite facings with variable in-plane or through the thickness properties (see for example, review by Birman and Byrd[1]);

3. Facings with a variable nonconventional geometry that could be called "sculptured" facings.

Sculptured facings can be designed in a number of ways, but the goal is always to increase the stiffness, either locally at the location of highest bending stress couples or over the entire facing. Two possible designs are facings with a piece-wise thickness distribution shown in Fig. 1 and ribbed facings with spaced stringers either embedded within the polymeric core or separating honeycomb sections placed in the space between the facings and the stringers[2]. In the present paper, we concentrate on the former design referred to as stepped facings. It should be noted that research on sandwich structures with a variable thickness has been conducted since the eighties[3-10]. However, these studies were concerned with tapered structures with a variable thickness of the core.

The panel with stepped facings shown in Fig. 1 can easily be manufactured using honeycomb or polymeric core sections of various depths. In the present paper we concentrate on the "global" response of the panel. The analysis of local stresses at the junction between sections of unequal facing thickness that may affect local strength of the panel is outside the scope of the paper. Note that these stresses become essential in the case of polymeric cores, while the relevant effect for honeycomb-core panels considered in the numerical analysis in this paper should be less prominent.

The purpose of this paper is to estimate potential advantages of sandwich panels with stepped facings in static bending, stability and vibration problems. The approach to the solution includes the analytical part based on the first-order shear deformation theory and a numerical finite element solution utilizing three-dimensional finite elements to model the core. The paper elucidates improvements in strength, stiffness and fundamental frequencies achieved using stepped facings, while accounting for the detrimental weight increase. This analysis results in conclusions on the desirability and feasibility of stepped facings. It is also shown that the first-order theory may be sufficiently accurate for the numerical analysis of panels with metallic honeycomb cores if they are not subject to local loads.

II. Analysis: Analytical Formulation

The formulation of the problem for sandwich panels with piece-wise facings is based on the first-order shear deformation theory[11]. This is justified since aerospace panels presently considered for such applications are relatively thin, so that the error produced by neglecting higher-order effects associated with warping of cross sections during deformation is negligible. The first-order theory was shown to yield accurate results for relatively slender sandwich panels if used with correct values of the shear correction

coefficients[12]. It is usually accepted that the assumptions of the first-order shear deformation theory are sufficiently accurate for sandwich structures with a relatively stiff core[13].

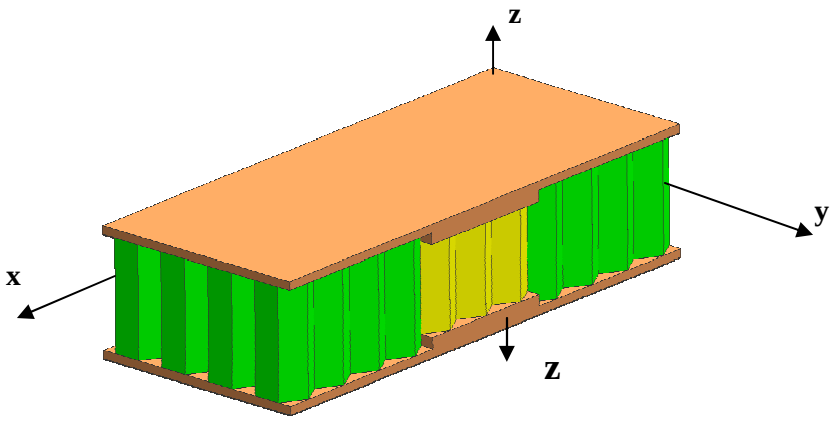

Figure 1: Honeycomb sandwich panel with stepped facings. The central section of the panel has thicker facings providing locally higher stiffness.

It is necessary to emphasize that the first-order theory is definitely unacceptable for studies of problems involving local loads where three-dimensional state of stress may be prevalent. For example, this theory would lead to serious mistakes if applied to the local stress analysis in the vicinity of bolts used to fasten the panel. In general, local stresses close to any discontinuity in the sandwich structure should be investigated by a higher-order theory or by a three-dimensional theory of elasticity or plasticity (the latter theory may be needed if the facings are manufactured from ductile metal matrix composites or metals). The other area where the first-order theory cannot be employed is found in sandwich structures with a "soft" core. While a detailed discussion of the subject of sandwich structures with a soft core is outside the scope of this paper, interested readers are referred to a number of recent references on the subject[13-15].

As follows from the previous paragraph, limitations superimposed on the use of the first-order theory are mostly irrelevant to problems considered in this paper that are concerned with a "global" response of sandwich panels. Moreover, panels considered in the present study have an aluminum honeycomb core that cannot be characterized as "soft." The validity of the theory will further be proven by a comparison of the results with those generated by FEA using three-dimensional finite elements. In addition to the assumptions of the first-order theory, the problem considered here is assumed geometrically linear. This is justified since sandwich panels found in typical aerospace applications fail at deflections that are smaller than the values necessitating the use of a geometrically nonlinear theory.

The solution of the static bending problem for a stepped panel simply supported along the straight edges $x = 0,\ a,\ y = 0,\ b$ and subjected to a lateral pressure $q(x, y)$ was obtained by the Rayleigh-Ritz method representing the potential energy as

$$\Pi = \frac{1}{2}\sum_{i,j}\int_{x_i}^{x_{i+1}}\int_{y_j}^{y_{j+1}}\int_{-h/2}^{h/2} u(x,y,z)\,dxdydz - \int_0^a\int_0^b q(x,y)w(x,y)\,dxdy \qquad (1)$$

where $u(x,y,z)$ is a strain energy density, and $x_i \le x \le x_{i+1},\ y_j \le y \le y_{j+1}$ identify a section with constant facing thickness. The sum in the first term in the right side of (1) integral includes all sections of the panel. The integration in (1) is conducted throughout the thickness, accounting both for the contribution of the strain energy associated with in-plane bending stresses in the facings as well as for the transverse shear strain energy accumulated in the core.

The strain energy density of a material in the three-dimensional state of stress in the Cartesian coordinate system is

$$u = \frac{1}{2}\left(\sigma_x\varepsilon_x + \sigma_y\varepsilon_y + \sigma_z\varepsilon_z + \tau_{xy}\gamma_{xy} + \tau_{xz}\gamma_{xz} + \tau_{yz}\gamma_{yz}\right) \tag{2}$$

The stress-strain relationships for a generally orthotropic material relate the tensor of stresses to the tensor of strains[11]:

$$\begin{Bmatrix}\sigma_x\\ \sigma_y\\ \sigma_z\\ \tau_{yz}\\ \tau_{xz}\\ \tau_{xy}\end{Bmatrix} = \begin{bmatrix} C_{11} & C_{12} & C_{13} & 0 & 0 & C_{16}\\ C_{12} & C_{22} & C_{23} & 0 & 0 & C_{26}\\ C_{13} & C_{23} & C_{33} & 0 & 0 & C_{36}\\ 0 & 0 & 0 & C_{44} & C_{45} & 0\\ 0 & 0 & 0 & C_{45} & C_{55} & 0\\ C_{16} & C_{26} & C_{36} & 0 & 0 & C_{66}\end{bmatrix}\begin{Bmatrix}\varepsilon_x\\ \varepsilon_y\\ \varepsilon_z\\ \gamma_{yz}\\ \gamma_{xz}\\ \gamma_{xy}\end{Bmatrix} \tag{3}$$

Following standard assumptions of the first order shear deformation theory the strains are the following functions of displacements and rotations:

$$\begin{aligned}
&\varepsilon_x = \frac{\partial u_0}{\partial x} + z\frac{\partial \psi_x}{\partial x}, \qquad \varepsilon_y = \frac{\partial v_0}{\partial y} + z\frac{\partial \psi_y}{\partial y}, \qquad \varepsilon_z = 0\\
&\gamma_{xy} = \frac{\partial u_0}{\partial y} + \frac{\partial v_0}{\partial x} + z\left(\frac{\partial \psi_x}{\partial y} + \frac{\partial \psi_y}{\partial x}\right)\\
&\gamma_{xz} = \frac{\partial w}{\partial x} + \psi_x, \qquad \gamma_{yz} = \frac{\partial w}{\partial y} + \psi_y
\end{aligned} \tag{4}$$

Sandwich panels considered in this paper are assumed to have symmetric cross-ply or multi-layered angle-ply facings. The honeycomb core is modeled using its equivalent stiffnesses so that it behaves as a homogeneous orthotropic material. Furthermore, the facings are symmetric about the middle plane of the panel, so that in-plane displacements are uncoupled from deflections and rotations. Then integrating the strain energy density of the sandwich panel throughout the thickness of the facings and the core and using equations (2), (3) and (4) we obtain

$$\Pi = \frac{1}{2}\sum_{i,j}\int_{x_i}^{x_{i+1}}\int_{y_j}^{y_{j+1}}\left[\begin{array}{l} D_{11}^{(ij)}\left(\frac{\partial \psi_x}{\partial x}\right)^2 + 2D_{12}^{(ij)}\frac{\partial \psi_x}{\partial x}\frac{\partial \psi_y}{\partial y} + D_{22}^{(ij)}\left(\frac{\partial \psi_y}{\partial y}\right)^2 + D_{66}^{(ij)}\left(\frac{\partial \psi_x}{\partial y} + \frac{\partial \psi_y}{\partial x}\right)^2 \\ + kA_{55}^{(ij)}\left(\frac{\partial w}{\partial x} + \psi_x\right)^2 + kA_{44}^{(ij)}\left(\frac{\partial w}{\partial y} + \psi_y\right)^2 \end{array}\right] dxdy \qquad (5)$$

$$-\int_0^a\int_0^b qwdxdy$$

The solution can be obtained representing deflections and rotations in double Fourier series that satisfy both kinematic and static boundary conditions, irrespectively of the variations in the thickness of the facings:

$$\begin{aligned} w &= \sum_m\sum_n W_{mn}\sin\frac{m\pi x}{a}\sin\frac{n\pi y}{b} \\ \psi_x &= \sum_m\sum_n F_{mn}\cos\frac{m\pi x}{a}\sin\frac{n\pi y}{b} \\ \psi_y &= \sum_m\sum_n P_{mn}\sin\frac{m\pi x}{a}\cos\frac{n\pi y}{b} \end{aligned} \qquad (6)$$

The substitution of (6) into (5) and integration yields

$$\Pi = \frac{1}{2}\sum_{i,j}\sum_{m,k,n,r}\left[\begin{array}{l} \left(D_{11}^{(ij)}\frac{m\pi}{a}\frac{k\pi}{a}F_{mn}F_{kr} + 2D_{12}^{(ij)}\frac{m\pi}{a}\frac{r\pi}{b}F_{mn}P_{kr} + D_{22}^{(ij)}\frac{n\pi}{b}\frac{r\pi}{b}P_{mn}P_{kr}\right)A_{mnkr}^{(ij)} + \\ D_{66}^{(ij)}\left(\frac{n\pi}{b}\frac{r\pi}{b}F_{mn}F_{kr} + 2\frac{k\pi}{a}\frac{n\pi}{b}F_{mn}P_{kr} + \frac{m\pi}{a}\frac{k\pi}{a}P_{mn}P_{kr}\right)B_{mnkr}^{(ij)} + \\ kA_{55}^{(ij)}\left(\frac{m\pi}{a}\frac{k\pi}{a}W_{mn}W_{kr} + 2\frac{m\pi}{a}W_{mn}F_{kr} + F_{mn}F_{kr}\right)C_{mnkr}^{(ij)} + \\ kA_{44}^{(ij)}\left(\frac{n\pi}{b}\frac{r\pi}{b}W_{mn}W_{kr} + 2\frac{n\pi}{b}W_{mn}P_{kr} + P_{mn}P_{kr}\right)D_{mnkr}^{(ij)} \end{array}\right] - \qquad (7)$$

$$\sum_{m,n}W_{mn}\int_0^a\int_0^b q(x,y)\sin\frac{m\pi x}{a}\sin\frac{n\pi y}{b}dxdy$$

where

$$A_{mnkr}^{(ij)} = \int_{x_i}^{x_{i+1}}\int_{y_j}^{y_{j+1}}\sin\frac{m\pi x}{a}\sin\frac{k\pi x}{a}\sin\frac{n\pi y}{b}\sin\frac{r\pi y}{b}dxdy$$

$$B_{mnkr}^{(ij)} = \int_{x_i}^{x_{i+1}}\int_{y_j}^{y_{j+1}}\cos\frac{m\pi x}{a}\cos\frac{k\pi x}{a}\cos\frac{n\pi y}{b}\cos\frac{r\pi y}{b}dxdy$$

$$C_{mnkr}^{(ij)} = \int_{x_i}^{x_{i+1}} \int_{y_j}^{y_{j+1}} \cos\frac{m\pi x}{a}\cos\frac{k\pi x}{a}\sin\frac{n\pi y}{b}\sin\frac{r\pi y}{b}\,dxdy$$
$$D_{mnkr}^{(ij)} = \int_{x_i}^{x_{i+1}} \int_{y_j}^{y_{j+1}} \sin\frac{m\pi x}{a}\sin\frac{k\pi x}{a}\cos\frac{n\pi y}{b}\cos\frac{r\pi y}{b}\,dxdy \qquad (8)$$

The standard Rayleigh-Ritz procedure implies that $\frac{\partial \Pi}{\partial W_{mn}} = \frac{\partial \Pi}{\partial F_{mn}} = \frac{\partial \Pi}{\partial P_{mn}} = 0$ yielding the following system of algebraic equations for unknown amplitudes of harmonics in series (6):

$$\sum_{i,j}\sum_{k,r}\left[kA_{55}^{(ij)}\left(\frac{m\pi}{a}\frac{k\pi}{a}W_{kr} + \frac{m\pi}{a}F_{kr}\right)C_{mnkr}^{(ij)} + kA_{44}^{(ij)}\left(\frac{n\pi}{b}\frac{r\pi}{b}W_{kr} + \frac{n\pi}{b}P_{kr}\right)D_{mnkr}^{(ij)}\right] -$$
$$\int_0^a\int_0^b q(x,y)\sin\frac{m\pi x}{a}\sin\frac{n\pi y}{b}\,dxdy = 0$$
$$\sum_{i,j}\sum_{k,r}\left[\begin{array}{l}\frac{m\pi}{a}\left(D_{11}^{(ij)}\frac{k\pi}{a}F_{kr} + D_{12}^{(ij)}\frac{r\pi}{b}P_{kr}\right)A_{mnkr}^{(ij)} + D_{66}^{(ij)}\frac{n\pi}{b}\left(\frac{r\pi}{b}F_{kr} + \frac{k\pi}{a}P_{kr}\right)B_{mnkr}^{(ij)} + \\ kA_{55}^{(ij)}\left(\frac{k\pi}{a}W + F_{kr}\right)_{kr} C_{mnkr}^{(ij)}\end{array}\right] = 0 \qquad (9)$$
$$\sum_{i,j}\sum_{k,r}\left[\begin{array}{l}\frac{n\pi}{b}\left(D_{22}^{(ij)}\frac{r\pi}{b}P_{kr} + D_{12}^{(ij)}\frac{k\pi}{a}F_{kr}\right)A_{mnkr}^{(ij)} + D_{66}^{(ij)}\frac{m\pi}{a}\left(\frac{k\pi}{a}P_{kr} + \frac{r\pi}{b}F_{kr}\right)B_{mnkr}^{(ij)} + \\ kA_{44}^{(ij)}\left(\frac{r\pi}{b}W_{kr} + P_{kr}\right)D_{mnkr}^{(ij)}\end{array}\right] = 0$$

Upon the solution of the system of equations (9), the strains throughout the panel can be determined from (4) and the stresses from (3). If the maximum deflection of the panel exceeds its half-thickness, geometrically nonlinear terms should be included into formulation (in such case, the analysis should be conducted numerically). In the presence of local loads, such as pressure concentrated over a small area of the loaded facing, the present solution may provide global deformations and stresses. However, if the local load is large it is advisable to consider local deformations of the loaded facing and the sections of the core and the opposite facing in the loaded region. Besides, local geometrically nonlinear effects may result in an interaction between global and local deformations and stresses. Accordingly, such problems are better analyzed by numerical methods.

The solution shown above is concerned with static pressure. In the case of eigenvalue problems, i.e. buckling or free vibration, the approach is similar, but it is necessary to account for the contribution of relevant energy terms. For example, in the case of free vibrations, the amplitudes of harmonics in series (6) depend on time, while the last term in the right side of (5) has to be replaced with the kinetic energy:

$$K = \frac{1}{2}\sum_{i,j}\int_{x_i}^{x_{i+1}}\int_{y_j}^{y_{j+1}}\left[m\left(\frac{\partial w}{\partial t}\right)^2 + I\left(\left(\frac{\partial \psi_x}{\partial t}\right)^2 + \left(\frac{\partial \psi_y}{\partial t}\right)^2\right)\right]dxdy \qquad (10)$$

where

$$m = \int_z \rho(x, y, z)dz \qquad I = \int_z \rho(x, y, z)z^2 dz \tag{11}$$

III. Analysis: Finite Element Model and Numerical Results

The model of the panel was developed using Nastran-2005. The facings were modeled by 2-D shell elements, while the core consisted of 3-D solid elements. The material of the cross-ply symmetric facings was laminated carbon/epoxy (T300/5208). The aluminum (AL-5056) honeycomb core was hexagonal with the foil thickness equal to 0.001 inch (for the equivalent properties of the core, see www.helcel.com).

First, the analytical solution for various conventional panel geometries (facings of constant thickness) was compared to the FEA result to verify the accuracy of the model. The size of panels considered in this comparison is listed in Table 1 (in-plane dimensions in this comparison differed from those referred to above). The width-to-thickness ratio equal to 20 was maintained in all cases. The facings were symmetric and cross-ply laminated $[0^o/90^o/0^o/90^o]_s$. The thickness of each layer in the facings of panels considered in this study was equal to 0.127 mm ($0.005''$). The panels were loaded by a uniform pressure equal to 50 psi. The fact that numerical and analytical solutions were in close agreement, even for such small size-to-thickness ratio, can be attributed to the honeycomb core being relatively "stiff." Furthermore, the stresses in the compressed facing of an 8-layer facing panel that is 254 mm ($10''$) long, 127 mm ($5''$) wide and 25.4 mm ($1''$) thick and subject to a uniform pressure equal to 350 psi were calculated by the first-order theory and compared to the 3-D finite element solution (Table 2). As follows from this table, the error associated with the first-order theory increases in the layers that are close to the core. However, even at the width-to-thickness ratio equal to 5, this error remains relatively small. Thus, the analytical solution for metallic honeycomb-core panels with the width-to-thickness ratio equal to or exceeding 20 probably does not have to rely on theories accounting for a "soft" core, with the exception of the case of high local loads.

The following results were generated using FEA since the accuracy of the first-order theory for sandwich panels with stepped facings requires further investigations. The panels were 254 mm ($10''$) long, 127 mm ($5''$) wide and 25.4 mm ($1''$) thick. Each facing of a "conventional" panel referred to below included 8 cross-ply layers. The facings of stepped panels included the central 12-layer $7.5'' * 2.3''$ section, adjacent 8-layer section with the outer dimensions $8.5'' * 3.5''$ and the outer 6-layer section. The weight of the stepped panel was only 5.7% larger than that of the conventional counterpart. The bending load applied to the panel in all examples, except for the buckling and free vibration analyses, was represented by a uniform static pressure equal to 2.413 MPa (350 psi).

The shapes of the conventional and stepped panels undergoing a uniform static pressure are shown in Fig. 2. The contours of bent panels are depicted in Figs. 3 and 4. As follows from these figures, the mode shapes of panels subject to static pressure are little affected by the stepped facing design. This implies that analytical solutions for such panels may employ mode shapes of deformation, buckling and free vibrations determined for their conventional counterparts.

A distribution of strains throughout the thickness of the panel with stepped facings obtained by FEA is shown in Fig. 5. As follows from this figure, the axial strains in the x-direction along the longer edges (ε_x) are nearly linearly distributed through the thickness. However, their counterparts in the y-direction (ε_y) deviate from the linear distribution reflecting a small width-to-thickness ratio equal to 5.

Evidently, the panels with such size-to-thickness ratio should be investigated using a higher-order theory or numerical FEA 3-D models. It is interesting to note that while the strain in the y-directions is a nonlinear function of the thickness coordinate, a classical third-order theory would probably be insufficient to accurately represent its through-the-thickness distribution.

The effect of the stepped facing design on the strains and stresses in the facings compared to those in the conventional panel is depicted in Figs. 6 and 7. As shown in Fig. 6, the axial strains in the facings in both x- and y-directions are significantly reduced using stepped facings. Axial stresses in the facings are also noticeably reduced by redistributing the material as follows from Fig. 7. Note that while the strains are continuous functions of the thickness coordinate the stresses in the facings change abruptly from layer to layer (this is evident in Fig. 7). This reflects a much higher stiffness of layers in the fiber direction.

Table 1. Maximum deflections in conventional panels with the width-to-thickness ratio equal to 20 by the analytical first-order theory solution and 3-D FEA.

Panel No.	Length in the x-direction (a), inch.	Width in the y-direction (b), inch.	Thickness (h), inch.	Depth of honeycomb core, inch.	Max. deflection by first-order theory, inch.	Max. deflection by 3-D FEA, inch
1	20	10	0.5	0.42	0.176	0.169
2	24	12	0.6	0.52	0.232	0.224
3	28	14	0.7	0.62	0.296	0.287
4	32	16	0.8	0.72	0.368	0.358
5	36	18	0.9	0.82	0.447	0.436
6	40	20	1	0.92	0.535	0.522

Table 2. Maximum stresses in the layers of the compressed facing of a conventional panel (10″ long, 5″ wide and 1″ deep) by the analytical first-order theory solution and 3-D FEA.

Layer (from surface to core)	Orientation of layer, deg.	Analytical σ_x (ksi)	FEA σ_x (ksi)	Difference between analytical and FEA deflections, %	Analytical σ_y (ksi)	FEA σ_y (ksi)	Difference between analytical and FEA deflections, %
8	0	38.989	38,752	1.08	3.644	3.673	0.8
7	90	2.866	2.935	2.34	51.137	52.533	2.66
6	0	38.208	37.588	1.65	3.294	3.394	2.95
5	90	2.807	2.809	0.07	47.452	47.842	0.82
4	90	2.779	2.746	1.2	44.555	45.497	2.07
3	0	37.039	36.112	2.57	3.041	2.975	2.22
2	90	2.72	2.62	3.8	43.627	40.806	6.91
1	0	36.259	35.128	3.22	2.977	2.696	10.44

Note: The sign minus indicating compression is omitted.

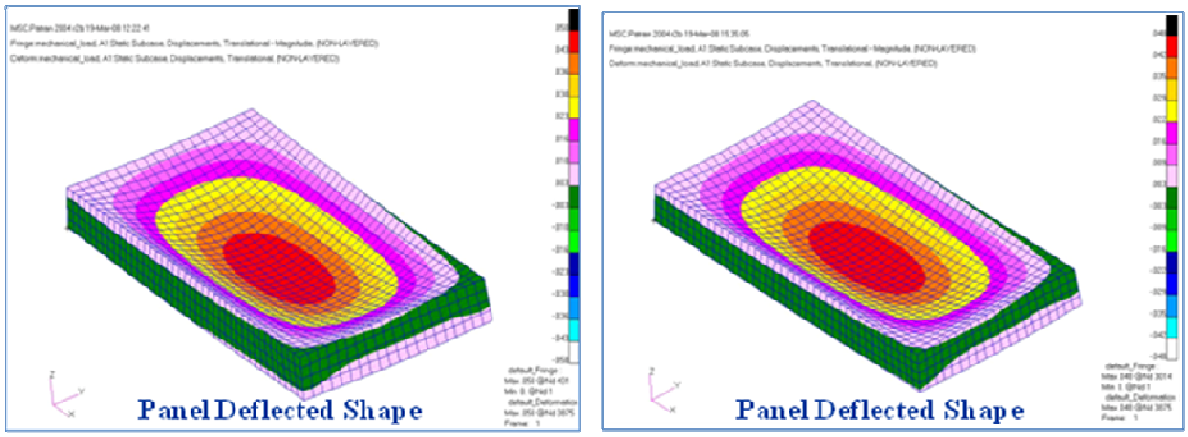

Figure 2. Shape of conventional (left) and Stepped (right) panels undergoing bending due to a uniform pressure.

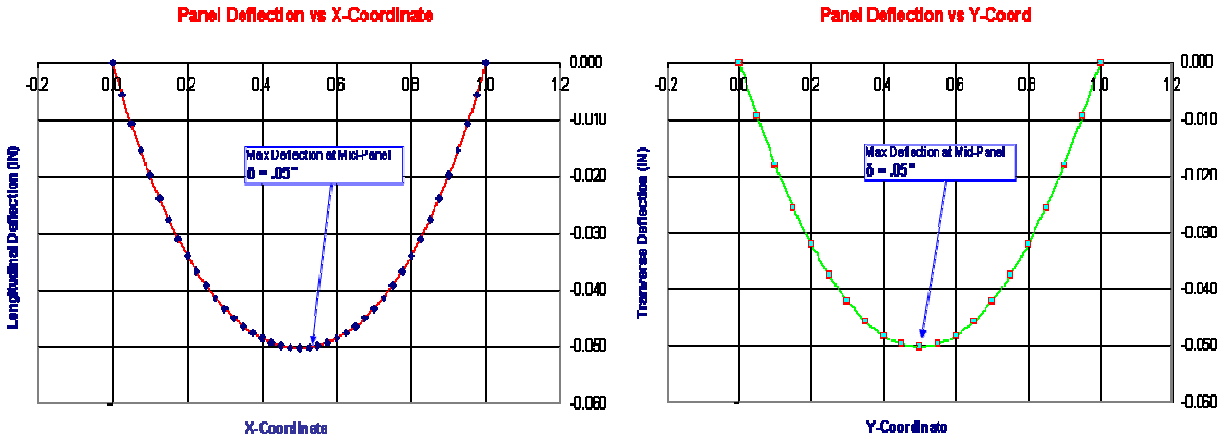

Figure 3. Mode shape of deflections of the conventional panel subject to a uniform pressure. The horizontal axes show nondimensional x- and y-coordinates normalized with respect to the corresponding dimension.

The comparison between the compressive stresses and strains at the center of the conventional (8-layer facings) and stepped panels is also shown in Tables 3 and 4. This comparison is limited to the top facing that experiences compression as a result of bending. Note that while the tensile strains in the opposite facings have the same absolute value as those in the corresponding layers in the top facing, the stresses in the facings differ reflecting a difference in the tensile and compressive moduli of the facing material. As follows from Figs. 6 and 7 and from Tables 3 and 4, a reduction in maximum stresses in the 0^o-layers oriented in the x-direction reaches 12.9% in the fiber direction and 20.2% in the direction perpendicular to the fibers. For 90^o-layers oriented in the y-direction the corresponding improvements in the maximum stress are 22.3% and 15.5%, respectively. The axial strains in the x-direction are also reduced by almost 13%. These improvements achieved at the cost of a small weight increase (5.7%) indicate that the use of stepped facings may be an attractive option in designs where the strength of the panel is the dominant factor. Shear stresses in the core do not represent the mode of failure for the panel under consideration; hence they are not discussed here.

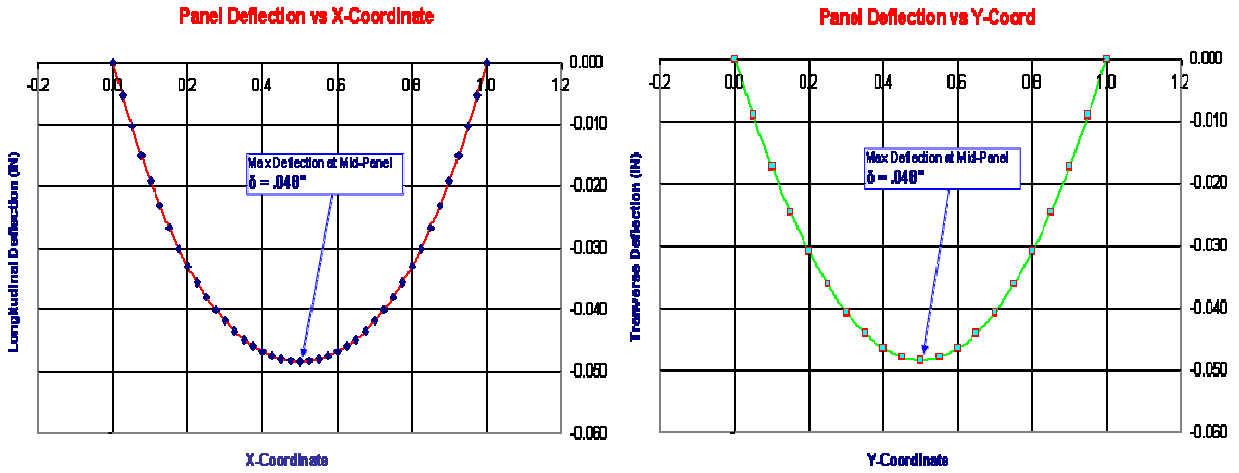

Figure 4. Mode shape of deflections of the stepped panel subject to a uniform pressure. The horizontal axes show nondimensional x- and y-coordinates normalized with respect to the corresponding dimension.

Buckling resistance of stepped panels is also improved by the stepped facing design. This was shown analyzing the panel subject to a uniform compression along the x-axis. The same stepped design as that described above resulted in an increase of the buckling load by 11.7% (from 3690 lbs to 4120 lbs). The increase in the fundamental frequency was less pronounced as it increased by only 9.5%, from 3432 Hz for the conventional panel to 3759 Hz for the stepped counterpart. This smaller increase in the frequency is explained by the higher fraction of the mass of the stepped panel that is concentrated at the center, reducing the beneficial effect of a locally improved stiffness. Note that both in the static buckling as well as in the free vibration problems, the shape of the deformed panel was dominated by the first mode shape of deformation, i.e. one half-wave of deformation in both x and y directions as evidenced in Fig. 8.

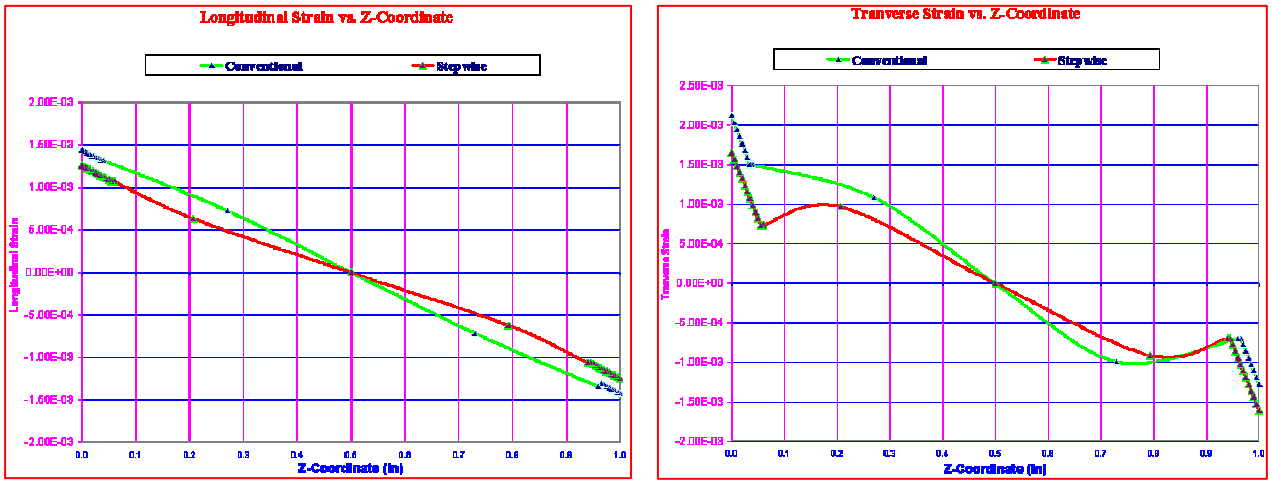

Figure 5: Distribution of axial strains throughout the thickness of stepped panels obtained by FEA (Left case: strains in the x-direction, right case: strains in the y-direction).

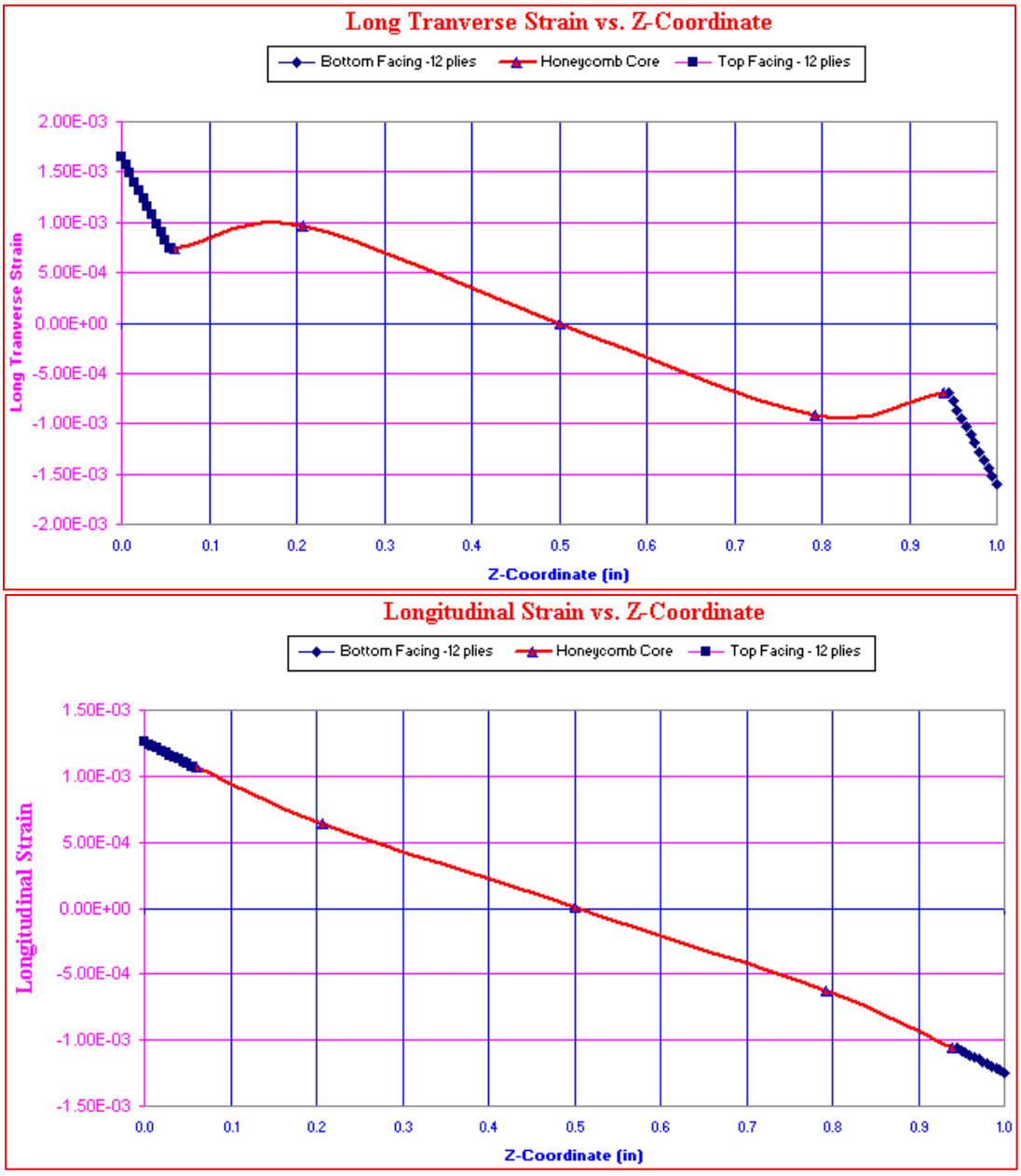

Figure 6: Distribution of axial strains throughout the thickness of stepped panels obtained by FEA (Top case: strains in the x-direction, bottom case: strains in the y-direction).

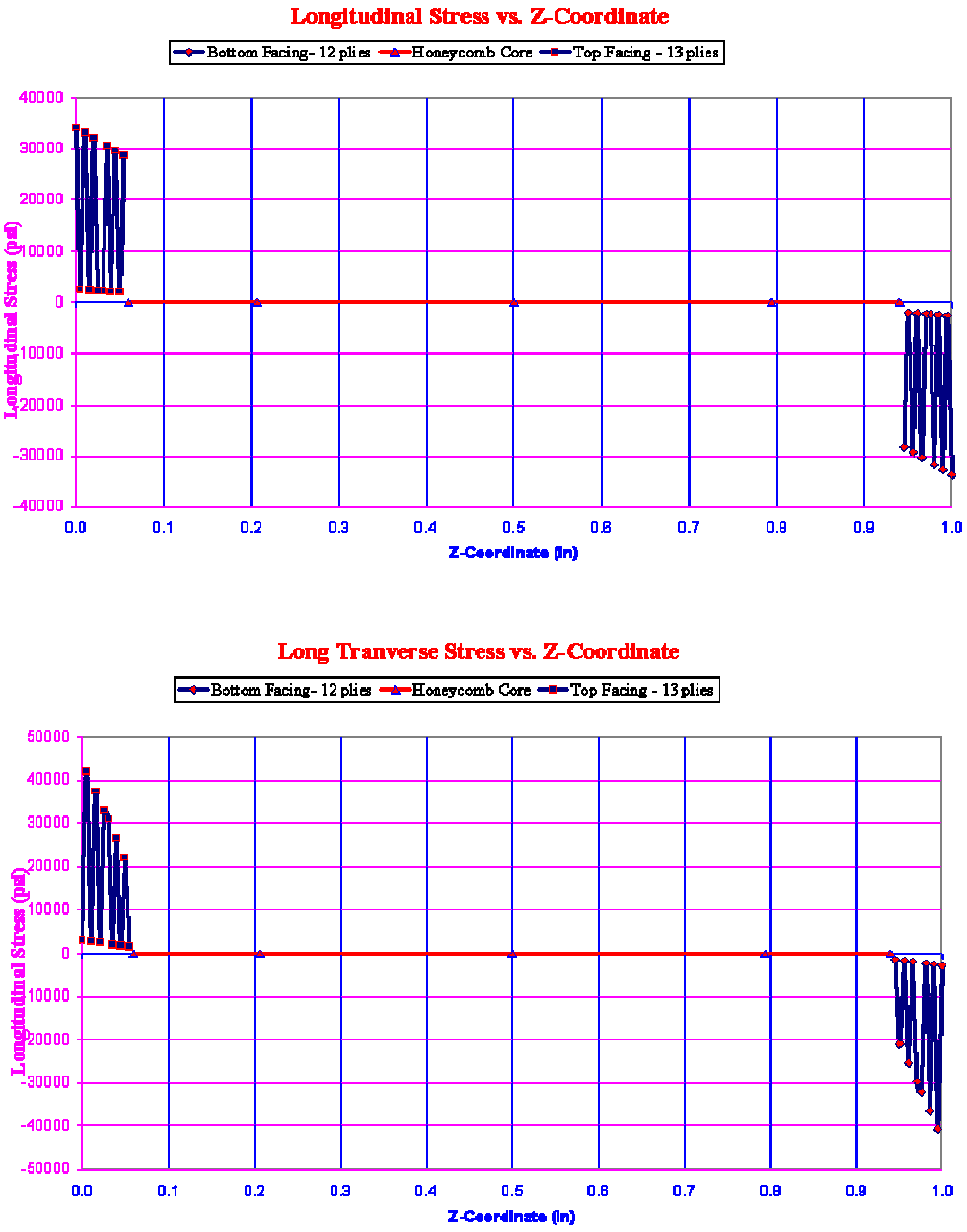

Figure 7: Distribution of axial stresses throughout the thickness of stepped panels obtained by FEA. (Top case: stresses in the x-direction, bottom case: stresses in the y-direction).

Table 3. Stresses and strains at the center of the upper (compressed) facing of the conventional sandwich panel.

Layer	Orientation of layer, deg.	z (inch)	σ_x (ksi)	σ_y (ksi)	$\varepsilon_x * (10^3)$	$\varepsilon_y * (10^3)$
8	0	1.000	38.572	3.673	1.430	1.280
7	90	0.995	2.935	52.533	1.410	1.190
6	0	0.900	37.588	3.394	1.390	1.110
5	90	0.985	2.809	47.842	1.380	1.030
4	90	0.980	2.746	45.497	1.360	0.944
3	0	0.975	36.112	2.975	1.340	0.861
2	90	0.970	2.620	40.806	1.320	0.778
1	0	0.965	35.128	2.696	1.310	0.695

Notes: The sign minus indicating compression is omitted. The coordinate of the upper surface of the corresponding layer is shown in the third column.

Table 4. Stresses and strains at the center of the upper (compressed) facing of the conventional sandwich panel.

Layer	Orientation of layer, deg.	z (inch)	σ_x (ksi)	σ_y (ksi)	$\varepsilon_x * (10^3)$	$\varepsilon_y * (10^3)$
12	0	1.000	33.615	2.930	1.250	1.610
11	90	0.995	2.480	40.821	1.230	1.530
10	0	0.990	32.658	2.668	1.210	1.440
9	90	0.985	2.361	36.415	1.200	1.360
8	0	0.980	31.701	2.405	1.180	1.280
7	90	0.975	2.241	32.010	1.160	1.190
6	0	0.970	2.181	29.807	1.150	1.110
5	90	0.965	30.266	2.010	1.130	1.030
4	0	0.960	2.061	25.402	1.110	0.944
3	90	0.955	29.309	1.748	1.100	0.861
2	0	0.950	1.941	20.997	1.080	0.778
1	90	0.945	28.353	1.485	1.060	0.695

Notes: The sign minus indicating compression is omitted. The coordinate of the upper surface of the corresponding layer is shown in the third column.

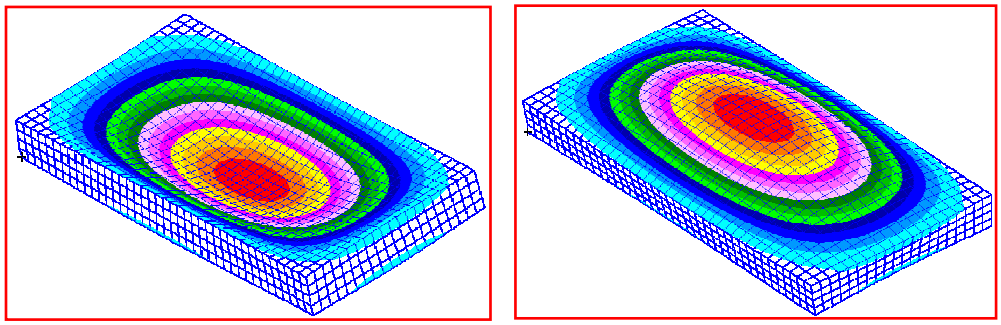

Figure 8: Mode shape of free vibrations of conventional and stepped panels. (Left case: conventional panel, right case: stepped panel)

IV. Conclusions

A potential for design of sandwich panels with stepped facings has been investigated. It appears that while stepped facings may lead to a slightly heavier structure, they provide a significant benefit reducing bending stresses in the facings. Such design may also prove advantageous for structures where the mode of failure is buckling. If the goal is to increase the fundamental frequency, stepped facings are less promising as a larger weight of the central part of the panel becomes detrimental, reducing or eliminating the advantages due to a locally improved stiffness. Overall, it is obvious that sandwich structures with stepped facings may be an attractive alternative to the conventional design, particularly in static problems. This conclusion is reinforced by the observation that the manufacture of such panels does not involve significant complications compared to conventional sandwich structures. A further research might concentrate on the optimization of the stepped design aiming at achieving desirable strength or stiffness subject to prescribed weight limitations.

In addition, the feasibility of using solutions based on the first-order theory for the analysis of sandwich panels with a commercially available aluminum honeycomb core was considered to address the observations that this theory is inaccurate in the case of a "soft" core. As was shown through the comparison of deflections and stresses generated by the analytical first-order theory solution with finite element results accounting for three-dimensional effects, the theory remains sufficiently accurate, even at the width-to-thickness ratio equal to 20. Therefore, it is concluded that commercially available honeycomb cores will often be "stiff enough" to justify the application of the first-order theory to the analysis of typical sandwich structures. This observation may become invalid in the case of panels with a "softer" polymeric core or in the case of concentrated loads resulting in local three-dimensional effects.

Acknowledgement

This research was supported by Boeing that provided necessary technical and computational resources. The discussions with Professor George A. Kardomateas (Georgia Institute of Technology) are warmly appreciated.

References

[1]Birman, V., and Byrd, L.W., "Modeling and Analysis of Functionally Graded Materials and Structures," *Applied Mechanics Reviews*, Vol. 60, 2007, pp. 195-216.

[2]Birman, V., Simitses, G.J., and Shen, L., "Stability of Short Sandwich Cylindrical Shells with Rib-Reinforced Facings", *Recent Advances in Applied Mechanics*, edited by J.T. Katsikadelis, D.E. Beskos and E.E. Gdoutos, National Technical University of Athens, Greece, 2000, pp. 11-21.

[3]Gupta, A.P., and Sharma, K.P., "Bending of a Sandwich Annular Plate of Variable Thickness," *Indian Journal of Pure and Applied Mathematics*, Vol. 13, 1982, pp. 1313-1321.

[4]Paydar, N., and Libove, C., "Stress Analysis of Sandwich Plates of Variable Thickness," *Journal of Applied Mechanics*, Vol. 55, 1988, pp. 419-424.

[5]Libove, C., and Lu, C.-H., "Beamlike Bending of Variable-Thickness Sandwich Plates," *AIAA Journal*, Vol. 12, 1989, pp. 1617-1618.

[6]Lu, C.-H., and Libove, C., "Beamlike Harmonic Vibration of Variable-Thickness Sandwich Plates," *AIAA Journal*, Vol. 29, 1991, pp. 299-305.

[7]Lu, C.-H., "Bending of Anisotropic Sandwich Beams with Variable Thickness," *Journal of Thermoplastic Composite Materials*, Vol. 7, 1994, pp. 364-374.

[8]Peled, D., and Frostig, Y., "High-Order Bending of Sandwich Beams with Variable Flexible Core and Nonparallel Skins," *ASCE Journal of Engineering Mechanics*, Vol. 120, 1994, pp. 1255-1269.

[9]Vel, S.S., Cacesse, V., and Zhao, H., "Modeling and Analysis of Tapered Sandwich Beams," *Proceedings of the American Society for Composites, Seventeenth Annual Technical Conference*, Purdue University, Fort Lafayette, Indiana, October 21-23, 2002.

[10]Vel, S.S., Cacesse, V., and Zhao, H., "Elastic Coupling Effects in Tapered Sandwich Panels with Laminated Anisotropic Composite Facings," *Journal of Composite Materials*, Vol. 39, 2005, pp. 2161-2183.

[11]Reddy, J.N., *Mechanics of Laminated Composite Plates and Shells*. *Theory and Analysis*, 2nd edition, CRC Press, Boca Raton, 2004.

[12]Noor, A.K., "Finite Element Buckling and Postbuckling Analyses," *Buckling and Postbuckling of Composite Plates*, edited by G.J. Turvey and I.H. Marshall, Chapman & Hall, London, 1995, pp. 58-107.

[13]Li, R., and Kardomateas, G.A., "Nonlinear High-Order Core Theory for Sandwich Plates with Orthotropic Phases," *AIAA Journal*, Vol. 46, 2008, pp. 2926-2934.

[14]Sokolinsky, V., and Frostig, Y., "Branching Behavior in the Nonlinear Response of Sandwich Panels with a Transversely Flexible Core," *International Journal of Solids and Structures*, Vol. 37, 2000, pp. 5745-5772.

[15]Frostig, Y., Thomsen, O.T., and Sheinman, I., "On the Non-Linear Theory of Unidirectional Sandwich Panels with a Transversely Flexible Core," *International Journal of Solids and Structures*, Vol. 42, 2005, pp. 1443-1463.